frontiers in Pharmacology

ORIGINAL RESEARCH
published: 17 January 2018
doi: 10.3389/fphar.2017.01001

Computational and Pharmacological Evaluation of Ferrocene-Based Acyl Ureas and Homoleptic Cadmium Carboxylate Derivatives for Anti-diabetic Potential

Shahar Bano[1], *Arif-ullah Khan*[1]*, *Faiza Asghar*[2,3], *Muhammad Usman*[2], *Amin Badshah*[2] *and Saqib Ali*[2]

[1] Riphah Institute of Pharmaceutical Sciences, Riphah International University, Islamabad, Pakistan, [2] Department of Chemistry, Quaid-e-Azam University, Islamabad, Pakistan, [3] Department of Chemistry, University of Wah, Wah, Pakistan

We investigated possible anti-diabetic effect of ferrocene-based acyl ureas: 4-ferrocenyl aniline (PFA), 1-(4-chlorobenzoyl)-3-(4-ferrocenylphenyl) urea (DPC1), 1-(3-chlorobenzoyl)-3-(4-ferrocenylphenyl) urea (DMC1), 1-(2-chlorobenzoyl)-3-(4-ferrocenylphenyl) urea (DOC1) and homoleptic cadmium carboxylates: bis (diphenylacetato) cadmium (II) (DPAA), bis (4-chlorophenylacetato) cadmium (II) (CPAA), using *in silico* and *in vivo* techniques. PFA, DPC1, DMC1, DOC1, DPAA and CPAA exhibited high binding affinities (ACE ≥ -350 Kcal/mol) against targets: aldose reductase, peroxisome proliferator-activated receptor γ, 11β-hydroxysteroid dehydrogenase-1, C-alpha glucosidase and glucokinase, while showed moderate affinities (ACE ≥ -250 Kcal/mol) against N-alpha glucosidase, dipeptidyl peptidase-IV, phosphorylated-Akt, glycogen synthase kinase-3β, fructose-1,6-bisphosphatase and phosphoenolpyruvate carboxykinase, whereas revealed lower affinities (ACE < -250 Kcal/mol) vs. alpha amylase, protein tyrosine phosphatases 1B, glycogen phosphorylase and phosphatidylinositol 3 kinase. In alloxan (300 mg/Kg)-induced diabetic mice, DPAA and DPC1 (1–10 mg/Kg) at day 1, 5, 10, 15, and 20th decreased blood glucose levels, compared to diabetic control group and improved the treated animals body weight. DPAA (10 mg/Kg) and DPC1 (5 mg/Kg) in time-dependent manner (30–120 min.) enhanced tolerance of oral glucose overload in mice. DPAA and DPCI dose-dependently at 1, 5, and 10 mg/Kg decreased glycosylated hemoglobin levels in diabetic animals, as caused by metformin. These results indicate that aforementioned derivatives of ferrocene and cadmium possess anti-diabetic potential.

Keywords: ferrocene-based acyl ureas, homoleptic cadmium carboxylates, molecular docking, anti-diabetic, mice

OPEN ACCESS

Edited by:
Ajay Sharma,
Chapman University, United States

Reviewed by:
Cesario Bianchi,
University of Mogi das Cruzes, Brazil
Francesco Pappalardo,
Università degli Studi di Catania, Italy

***Correspondence:**
Arif-ullah Khan
arif.ullah@riphah.edu.pk

Specialty section:
This article was submitted to Experimental Pharmacology and Drug Discovery, a section of the journal Frontiers in Pharmacology

Received: *02 November 2017*
Accepted: *29 December 2017*
Published: *17 January 2018*

Citation:
Bano S, Khan A, Asghar F, Usman M, Badshah A and Ali S (2018) Computational and Pharmacological Evaluation of Ferrocene-Based Acyl Ureas and Homoleptic Cadmium Carboxylate Derivatives for Anti-diabetic Potential. Front. Pharmacol. 8:1001. doi: 10.3389/fphar.2017.01001

INTRODUCTION

Diabetes mellitus (DM) is foremost health disorder, growing frequently in developing countries. Factors responsible for DM include increased deskbound lifestyle, nutrition changeover and rapid urbanization leading to widespread, parallel to rise in obesity (Hu, 2011). According to WHO, the 7th chief cause of deaths in 2030 will be DM (Mathers and Loncar, 2006). DM is

mainly characterized by high blood glucose levels, i.e., hyperglycemia with altered metabolism of carbohydrates, proteins and fats due to reduced insulin secretions or/and insulin action. Type I diabetes is associated with deficiency of insulin due to autoimmune-mediated β cells damage (Tuomi, 2005). Hyperglycemic condition in type I diabetes is controlled by administering exogenous insulin via subcutaneous route. However, type II diabetes is associated with relatively reduced levels or/and reduced sensitivity of hepatic, cardiac and fat cell toward insulin action. Thus, patients with type II diabetes rely on synthetic anti-diabetic therapy (Nathan et al., 2009).

Until now, many of the metals have been reported to possess anti-diabetic potential, such as vanadium (Heyliger et al., 1985), chromium (Anderson et al., 1997), cobalt (Ybarra et al., 1997), molybdenum (Ozcelikay et al., 1996), tungsten (Barberà et al., 2001), cadmium (Gümüşlü et al., 1997), iron, and copper (Siva and Kumar, 2013). Ferrocene derivatives containing iron moiety have been reported for good binding affinity to DNA, having cytotoxic, anticancer, antimalarial, antibiotic and antiviral activities (Lal et al., 2011; Asghar et al., 2017). Acyl urea group possesses anticancer, anticonvulsant, antimicrobial and antioxidant activities. Acyl urea derivatives have also been reported for anti-diabetic effect by inhibition of human liver glycogen phosphorylase (Klabunde et al., 2005). High levels of selenium in serum are associated with DM prevalence (Bleys et al., 2007). Cadmium is responsible for decrease in plasma selenium levels in alloxane treated diabetic rats (Gümüşlü et al., 1997). Carboxylate complexes with tin have been reported for α-glucosidase inhibition (Roy et al., 2015).

In present study, we made an effort to explore anti-diabetic potential of ferrocene and cadmium selected derivatives including 4-ferrocenyl aniline (PFA), 1-(4-chlorobenzoyl)-3-(4-ferrocenylphenyl) urea (DPC1), 1-(3-chlorobenzoyl)-3-(4-ferrocenylphenyl) urea (DMC1), 1-(2-chlorobenzoyl)-3-(4-ferrocenylphenyl) urea (DOC1), bis (diphenylacetato) cadmium (II) (DPAA), and bis (4-chlorophenylacetato) cadmium (II) (CPAA), through molecular docking and *in vivo* animals experimentation models. The chemical structures of test compounds were drawn via Chem. Sketch 2015 2.5 (**Figure 1**).

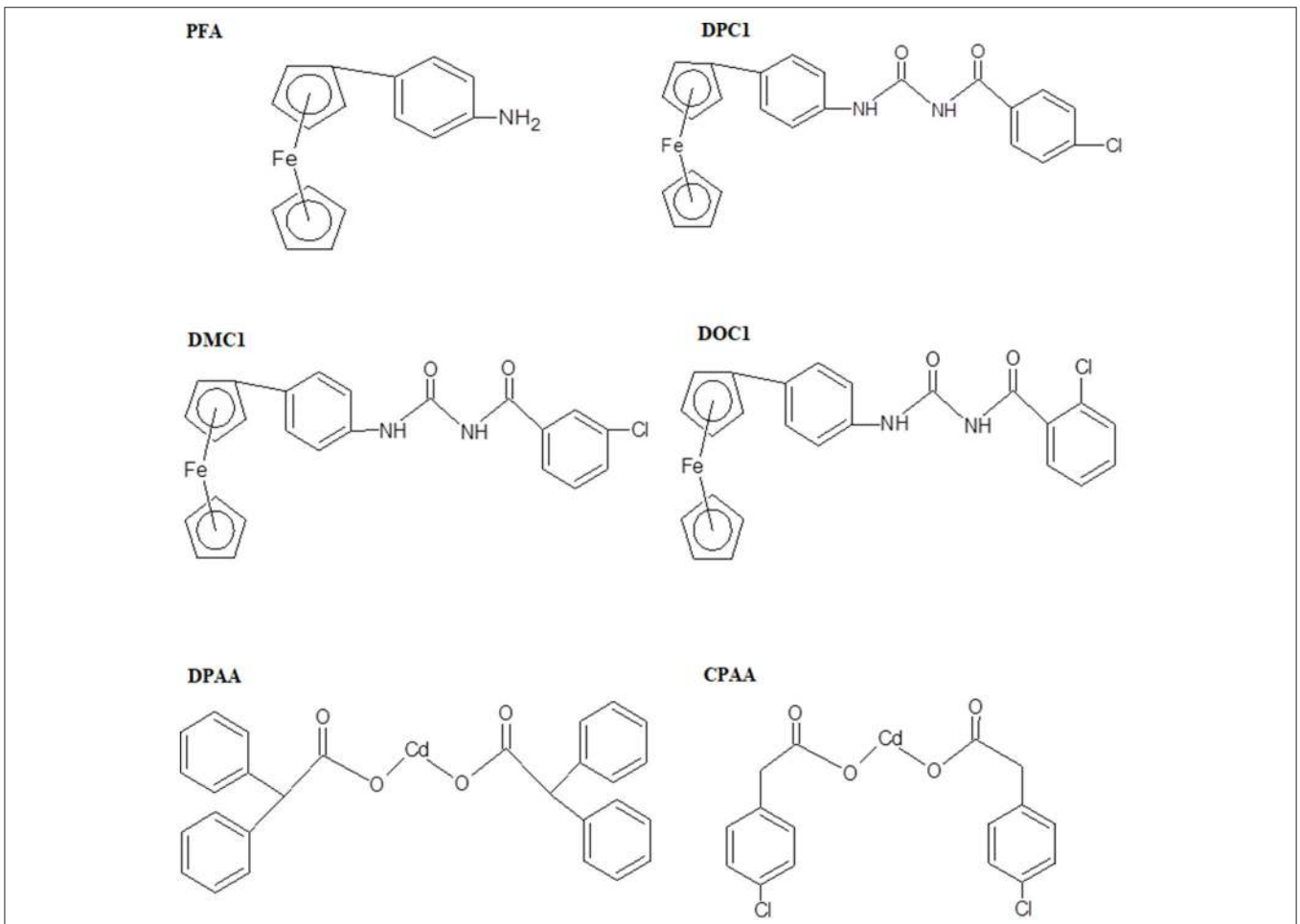

FIGURE 1 | Chemical structures of ferrocene incorporated acyl ureas and homoleptic cadmium carboxylates: 4-ferrocenyl aniline (PFA), 1-(4-chlorobenzoyl)-3-(4-ferrocenylphenyl) urea (DPC1), 1-(3-chlorobenzoyl)-3-(4-ferrocenylphenyl) urea (DMC1), 1-(2-chlorobenzoyl)-3-(4-ferrocenylphenyl) urea (DOC1), bis (diphenylacetato) cadmium (II) (DPAA), and bis (4-chlorophenylacetato) cadmium (II) (CPAA), drawn through Chem. Sketch 2015 2.5 software.

MATERIALS AND METHODS

Chemicals

Alloxan monohydrate and dimethyl sulphoxide (DMSO) were purchased from Sigma-Aldrich Co. LLC, U.S.A. Metformin HCL was obtained from Caraway Pharmaceuticals, National Industrial Zone Rawat, Islamabad, Pakistan. Ferrocene incorporated acyl ureas and homoleptic cadmium carboxylates were gifted by the Department of Chemistry, Quaid-e-Azam University. All chemicals were of analytical grade.

Animals

Adult Balb-C mice of either sex were kept under controlled temperature (22–25°C) at the animal house of Riphah Institute of Pharmaceutical Sciences, Islamabad, Pakistan. Animals were given free access to standard diet and water *ad libitum*. Experiments performed complied with rulings of Institute of Laboratory Animal Resources, Commission on Life Sciences University, National Research Council (1996), approved by Ethical Committee, Riphah Institute of Pharmaceutical Sciences (Ref. No.: REC/RIPS/2016/0013).

Docking Studies

3D-structures of the test compounds (PFA, DPC1, DMC1, DOC1, DPAA, and CPAA) were formed through Gauss View 5.0 software (**Figure 2**). 3D-structures of standard drug were obtained by converting 2D-structures through Biovia Discovery Studio Visualizer (DSV) 2016 (**Figure 3**). Polar hydrogen atoms (H-atoms) were added through same software, followed by saving into PDB format. Standard drugs were: miglitol, metformin, carbenoxolone, thiadiazolidinone-8 (TDZD-8), rosiglitazone, sitagliptin and ertiprotafib. 3D-structures of human protein targets involved in DM were retrieved from online data bank, RCSB PDB (https://www.rcsb.org/pdb/), as shown in **Figure 4**, according to their PDB IDs (Sussman et al., 1998). Target proteins were: alpha amylase (AA, PDB ID: 2QMK), C-alpha glucosidase (C-AG, PDB ID: 3TON), N-alpha glucosidase (N-AG, PDB ID: 2QMJ), aldose reductase (AR, PDB ID: 1US0), glucokinase (GK, PDB ID: IV4S), glycogen phosphorylase (GP, PDB ID: 1L7X), fructose-1,6-bisphosphatase (FBP1, PDB ID: 2JJK), phosphoenolpyruvate carboxykinase (PEPCK, PDB ID: 1KHB), 11β-hydroxysteroid dehydrogenase-1 (11β-HSD1, PDB ID: 2BEL), glycogen synthase kinase-3β (GSK-3β, PDB ID: 1Q4L), peroxisome proliferator-activated receptor γ (PPAR-γ, PDB ID: 2PRG), phosphatidylinositol 3 kinase (PI3K, PDB ID: 1E7U), phosphorylated-Akt (p-Akt, PDB ID: 3O96), dipeptidyl peptidase-IV (DPP IV, PDB ID: 2ONC), and protein tyrosine phosphatase 1B (PTP-1B, PDB ID: 2F70). By using same software, water molecules and ligands were removed and polar H-atoms were added, followed by saving in PDB format. Molecular

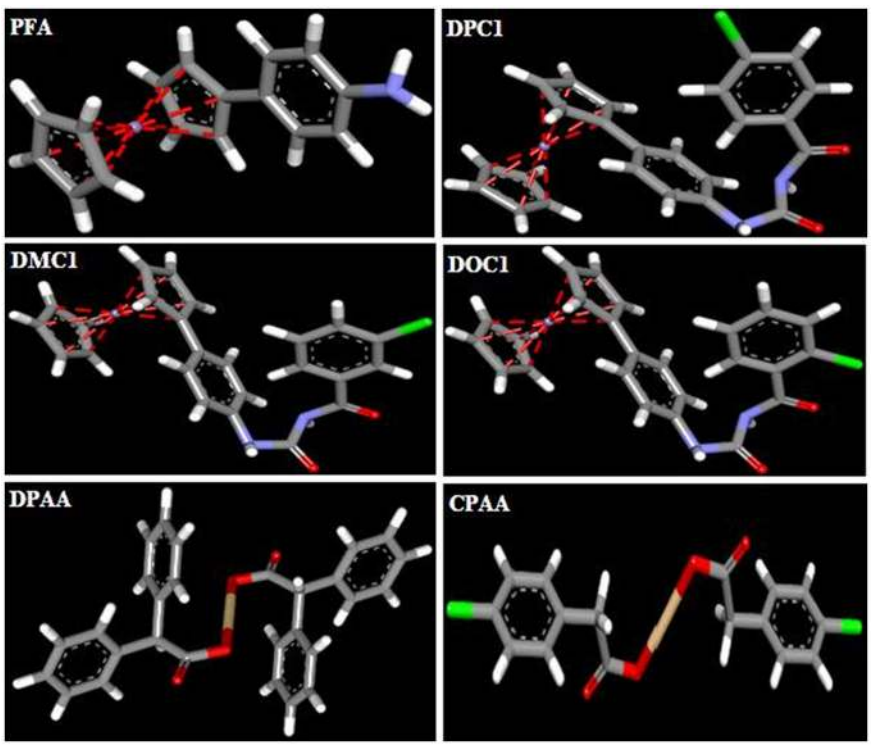

FIGURE 2 | 3D-structures of ferrocene incorporated acyl ureas and homoleptic cadmium carboxylates: 4-ferrocenyl aniline (PFA), 1-(4-chlorobenzoyl)-3-(4-ferrocenylphenyl) urea (DPC1), 1-(3-chlorobenzoyl)-3-(4-ferrocenylphenyl) urea (DMC1), 1-(2-chlorobenzoyl)-3-(4-ferrocenylphenyl) urea (DOC1), bis (diphenylacetato) cadmium (II) (DPAA), and bis (4-chlorophenylacetato) cadmium (II) (CPAA), drawn through Guass View 5.0 Software and saved into PDB format. Atoms are shown by colors; gray color (carbon atoms), white color (hydrogen atoms), red color (oxygen atoms), blue color (nitrogen atoms), yellowish color (cadmium atoms), and green color (chlorine atoms).

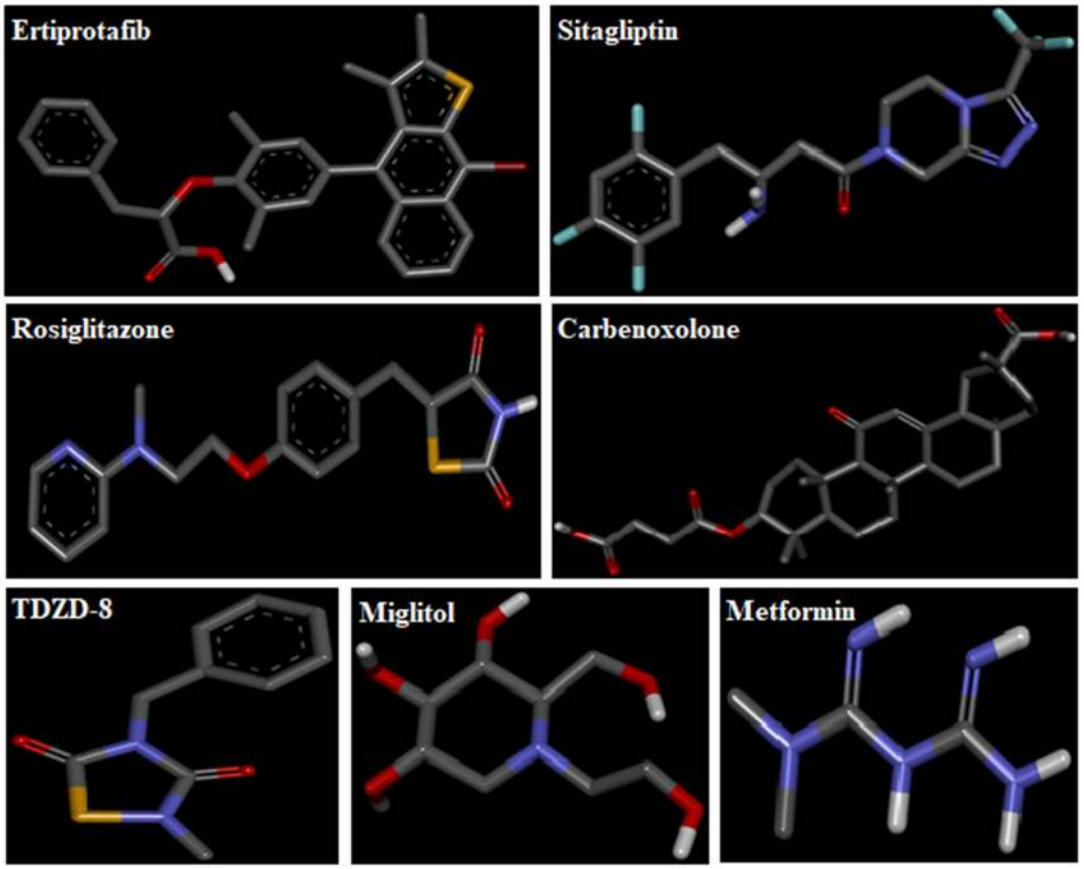

FIGURE 3 | 3D-structures of reference drugs: miglitol, metformin, carbenoxolone, thiadiazolidinone-8 (TDZD-8), rosiglitazone, sitagliptin and ertiprotafib, drawn through Chem. Sketch 2015 2.5 and saved in PDB format through Biovia Discovery Studio 2016. Atoms are shown by colors; gray color (carbon atoms), white color (hydrogen atoms), red color (oxygen atoms), blue color (nitrogen atoms), dark red (bromine), and yellow color (sulfur atoms).

docking was performed by PatchDock server, which is an online, geometry based automatic docking tool (Duhovny et al., 2002). We selected Root Mean Square Deviation clustering value at 2.0 to discard the redundant solutions of docking. Docking was executed and evaluated on bases of atomic contact energy (ACE) value (Kcal/mol) (Schneidman-Duhovny et al., 2005). Top 20 poses were evaluated and one with lowest ACE value (Kcal/mol) was selected for evaluation through Biovia DSV 2016. Each complex was assessed in 3D pattern to check the maximum binding interactions formed between ligands and amino acid residues including: alanine (ALA), arginine (ARG), asparagine (ASN), aspartic acid (ASP), cysteine (CYS), glutamine (GLN), glutamic acid (GLU), glycine (GLY), histidine (HIS), isoleucine (ILE), lysine (LYS), methionine (MET), phenylalanine (PHE), proline (PRO), serine (SER), threonine (THR), tryptophan (TRP), tyrosine (TYR), threonine (THR), and valine (VAL).

Blood Glucose Levels and Body Weight Measurement

Balb-C mice were adapted to the laboratory conditions and kept on overnight fasting (12–14 h). Alloxan was used for the induction of diabetes (Dunn and McLetchie, 1943). Solution of alloxan monohydrate (300 mg/Kg) was freshly prepared in saline and injected intra-peritoneally to mice (Bukhari et al., 2015). After 48 h, tail prick method was used to measure blood glucose levels of animals. Mice with blood glucose levels $\geq$200 mg/dL were considered as diabetic (Saudek et al., 2008). On basis of docking results, two most potential compounds were selected for *in vivo* studies. For DPAA and DPC1, animals were placed in six groups for each compound. The sample size in each group comprised of five mice. Group I and II were non-diabetic control and diabetic control, injected with saline (10 mL/Kg) and alloxan monohydrate (300 mg/Kg) respectively. Group III, IV, and V were alloxan-induced diabetic mice, administered with the test compound at doses of 1, 5, and 10 mg/Kg respectively. Group VI was positive control and injected with metformin (500 mg/Kg). Blood glucose levels were measured at day 1, 5, 10, 15, and 20th, using Easy Gluco auto-coding glucometer. For complete treatment period, body weight of animals was measured at same regular intervals.

Oral Glucose Tolerance Test (OGTT)

After keeping on 18 h fasting, mice were placed into four groups (for both compounds total eight groups). The sample size in

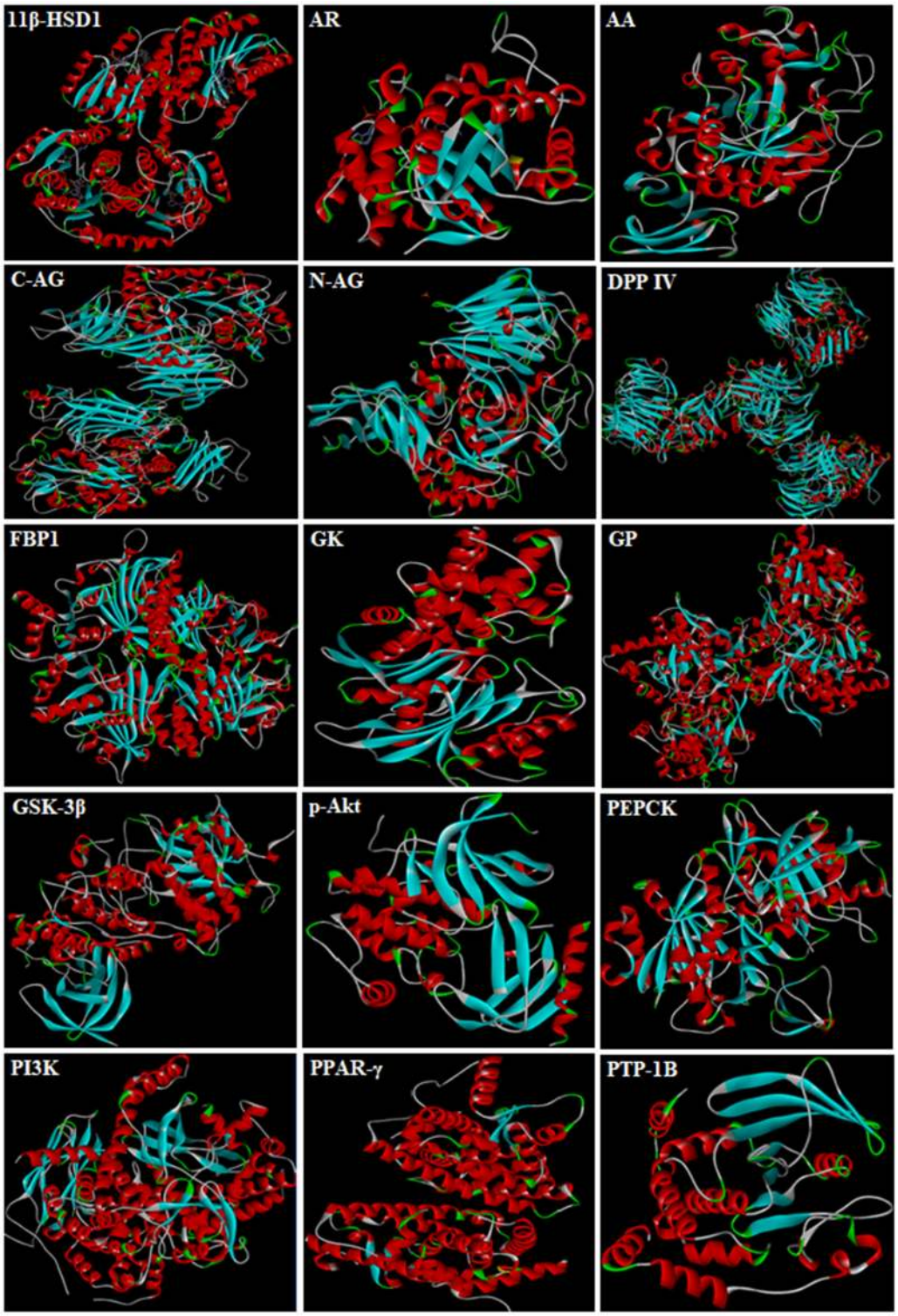

FIGURE 4 | 3D-structures of protein targets involved in diabetes: alpha amylase (AA), C-alpha glucosidase (C-AG), N-alpha glucosidase (N-AG), aldose reductase (AR), glucokinase (GK), glycogen phosphorylase (GP), fructose-1,6-bisphosphatase (FBP1), phosphoenolpyruvate carboxykinase (PEPCK), 11β-hydroxysteroid dehydrogenase-1 (11β-HSD1), glycogen synthase kinase-3β (GSK-3β), peroxisome proliferator-activated receptor γ (PPAR-γ), phosphatidylinositol 3 kinase (PI3K), phosphorylated-Akt (p-Akt), dipeptidyl peptidase-IV (DPP IV) and protein tyrosine phosphatase 1B (PTP-1B).

each group comprised of five mice. Group I and II were non-diabetic and diabetic control, injected with saline (10 mL/Kg) and alloxan (300 mg/Kg) respectively. Group III was treated with the test compound (DPAA, 10 mg/Kg/DPC1, 5 mg/Kg). Group IV was positive control and injected with metformin (500 mg/Kg). All groups were pre-treated and after 30 min. D-glucose load of 2 g/Kg was given orally. Blood glucose levels were measured at 0, 30, 60, 90, and 120 min., using Easy Gluco auto-coding glucometer (Marguet et al., 2000).

Glycosylated Hemoglobin (HbA1C) Test

After 6 weeks of treatment, HbA1C test was performed (Asgary et al., 2008) for all groups having sample size in each group comprised of five mice. Blood samples were collected using cardiac puncture method (Doeing et al., 2003). HbA1C level test carried out in Cantt Laboratory and Medical Imaging, Rawalpindi.

Acute Toxicity Test

Animals were kept on overnight fasting and distributed into different groups for each dose of DPAA (15, 25, 50, and 100 mg/Kg) and DPC1 (25, 50, and 100 mg/Kg). The sample size in each group comprised of five mice. After administration of compounds, animals were kept under observation for 7 days to determine mortality (Chen et al., 2009).

Statistical Analysis

Data expressed as mean ± standard error of mean (SEM). Significance of results was assessed by one-way analysis of variance (ANOVA), followed by *post-hoc* Tukey's test. $P < 0.05$ was deliberated to be statistically significant. The statistical assessment, preparation of graphs and evaluation was performed by using Graph Pad Prism 5.01.

RESULTS

Docking Evaluation

Docking evaluation was done by assessing ACE values, number of hydrogen bonds (H-bonds), number of π-π bonds and hydrophobic interactions formed between ligand-protein complexes. ACE (Kcal/mol) values for complexes of ligands and targets are shown in **Table 1**. Number of H-bonds and amino acids involved in making H-bonds are presented in **Table 2**. Number of π-π bonds and amino acids forming π-π bonds are expressed in **Table 3**. Hydrophobic interactions of best docked poses for ligand-protein complexes are plotted in **Table 4**. Interactions formed by DPAA, CPAA, PFA, DPC1, DMC1, DOC1 and standard drugs against AA, C-AG, N-AG, AR, GK, GP, FBP1, PEPCK, 11β-HSD1, GSK-3β, PPAR-γ, PI3K, p-Akt, DPP IV, and PTP-1B are shown in Figures S1–S15, respectively.

Effect on Blood Glucose Levels

At day 1, 5, 10, 15, and 20th, blood glucose levels of non-diabetic control (saline, 10 mL/Kg) group were 96 ± 4.11, 102 ± 3.74, 99 ± 2.44, 109 ± 3.63, and 114 ± 3.20 mg/dL respectively. Blood glucose levels of alloxan (300 mg/Kg) treated diabetic

TABLE 1 | ACE values (Kcal/mol) of best docked poses of 4-ferrocenyl aniline (PFA), 1-(4-chlorobenzoyl)-3-(4-ferrocenylphenyl) urea (DPC1), 1-(3-chlorobenzoyl)-3-(4-ferrocenylphenyl) urea (DMC1), 1-(2-chlorobenzoyl)-3-(4-ferrocenylphenyl) urea (DOC1), bis (diphenylacetato) cadmium (II) (DPAA), bis (4-chlorophenylacetato) cadmium (II) (CPAA) and standard drugs against alpha amylase (AA), C-alpha glucosidase (C-AG), N-alpha glucosidase (N-AG), aldose reductase (AR), glucokinase (GK), glycogen phosphorylase (GP), fructose-1,6-bisphosphatase (FBP1), phosphoenolpyruvate carboxykinase (PEPCK), 11β-hydroxysteroid dehydrogenase-1 (11β-HSD1), glycogen synthase kinase-3β (GSK-3β), peroxisome proliferator-activated receptor γ (PPAR-γ), phosphatidylinositol 3 kinase (PI3K), phosphorylated-Akt (p-Akt), dipeptidyl peptidase-IV (DPP IV) and protein tyrosine phosphatase 1B (PTP-1B).

Target proteins	PDB ID	Binding energies (ACE values Kcal/mol)						
		PFA	DPC1	DMC1	DOC1	DPAA	CPAA	Standard drugs
AA	2QMK	−177.77	−236.47	−231.29	−204.63	−277.18	−188.19	−131.81[A]
C-AG	3TON	−235.33	−397.72	−373.81	−374.69	−438.12	−301.76	−152.38[A]
N-AG	2QMJ	−260.19	−272.06	−320.05	−330.17	−369.10	−260.85	−249.33[A]
AR	1US0	−273.94	−383.49	−368.48	−387.05	−378.39	−286.37	−152.13[B]
GK	IV4S	−298.70	−426.22	−416.20	−412.65	−493.09	−299.26	−187.66[B]
GP	1L7X	−135.82	−206.36	−217.05	−243.26	−223.13	−198.71	−154.92[B]
FBP1	2JJK	−206.28	−341.22	−357.58	−344.46	−410.97	−151.99	−155.95[B]
PEPCK	1KHB	−196.02	−249.85	−302.87	−259.64	−292.61	−243.38	−152.17[B]
11β-HSD1	2BEL	−242.95	−388.87	−385.37	−377.20	−425.22	−278.48	−446.12[C]
GSK-3β	1Q4L	−204.83	−320.12	−253.96	−318.44	−343.95	−232.88	−209.66[D]
PPAR-γ	2PRG	−242.20	−361.51	−359.73	−340.37	−406.60	−273.52	−371.55[E]
PI3K	1E7U	−186.15	−195.32	−188.77	−210.48	−306.43	−254.74	−327.40[E]
p-Akt	3O96	−198.07	−272.81	−274.82	−288.05	−301.65	−176.69	−278.74[E]
DPP IV	2ONC	−133.07	−299.40	−299.99	−307.36	−273.27	−251.90	−171.61[F]
PTP-1B	2F70	−159.90	−215.85	−221.12	−147.93	−241.48	−170.28	−283.57[G]

Standard inhibitors or activator of pathways are: (A) miglitol, (B) metformin, (C) carbenoxolone, (D) thiadiazolidinone-8, (E) rosiglitazone, (F) sitagliptin, and (G) ertiprotafib.

TABLE 2 | Hydrogen bonds (H-bonds) formed by 4-ferrocenyl aniline (PFA), 1-(4-chlorobenzoyl)-3-(4-ferrocenylphenyl) urea (DPC1), 1-(3-chlorobenzoyl)-3-(4-ferrocenylphenyl) urea (DMC1), 1-(2-chlorobenzoyl)-3-(4-ferrocenylphenyl) urea (DOC1), bis (diphenylacetato) cadmium (II) (DPAA), bis (4-chlorophenylacetato) cadmium (II) (CPAA) and standard drugs against alpha amylase (AA), C-alpha glucosidase (C-AG), N-alpha glucosidase (N-AG), aldose reductase (AR), glucokinase (GK), glycogen phosphorylase (GP), fructose-1,6-bisphosphatase (FBP1), phosphoenolpyruvate carboxykinase (PEPCK), 11β-hydroxysteroid dehydrogenase-1 (11β-HSD1), glycogen synthase kinase-3β (GSK-3β), peroxisome proliferator-activated receptor γ (PPAR-γ), phosphatidylinositol 3 kinase (PI3K), phosphorylated-Akt (p-Akt), dipeptidyl peptidase-IV (DPP IV) and protein tyrosine phosphatase 1B (PTP-1B).

Proteins	PDB ID	PFA		DPC1		DMC1		DOC1		DPAA		CPAA		Standard drugs	
		H-bonds	Amino acids	H-bonds	Amino acids	H-bonds	Amino acids	H-bonds	Amino acids	H-bonds	Amino acids	H-bonds	Amino acids	H-bonds	Amino acids
AA	2QMK	2	GLY304 ILE312	1	ASP353	0	–	1	ASN352	1	ARG346	0	–	2^{A}	ILE312 THR314
C-AG	3TON	0	–	1	ASN1776	3	ASN1776 VAL1812 VAL1809	1	ASN1776	0	–	2	ASN1827 ASN1827	0^{A}	–
N-AG	2QMJ	0	–	2	SER120 SER120	0	–	5	ALA537 ILE523 PHE535 ARG520 SER521	1	SER288	0	–	2^{A}	GLY533 ALA536
AR	1US0	0	–	2	ALA299 CYS298	1	CYS303	0	–	0	–	1	TRP111	1^{B}	HIS110
GK	IV4S	0	–	0	–	0	–	1	ARG63	2	SER64 ALA456	0	–	1^{B}	VAL452
GP	1L7X	0	–	3	HIS377 ASN484 ASN484	1	HIS377	1	LYS680	3	THR676 GLY675 ARG569	0	–	3^{B}	GLY186 GLY186 TYR52
FBP1	2JJK	0	–	1	ALA189	0	–	1	ALA189	0	–	1	LYS72	3^{B}	GLY26 GLY26 MET18
PEPCK	1KHB	0	–	1	PRO337	1	VAL335	1	PHE530	1	ARG436	1	ASN292	0^{B}	–
11β-HSD1	2BEL	2	NAP1278 NAP1278	0	–	2	THR124 NAP1278	0	–	1	THR222	0	–	2^{C}	TYR177 TYR177
GSK-3β	1Q4L	1	ASN64	0	–	0	–	0	–	1	ASN95	1	ARG223	0^{D}	–
PPAR-γ	2PRG	1	MET348	0	–	0	–	0	–	0	–	1	SER289	0^{E}	–
PI3K	1E7U	0	–	2	THR1043 THR1043	1	ASP632	2	ASP632 ASN634	0	–	0	–	0^{E}	–
p-Akt	3O96	0	–	2	THR211 THR211	2	VAL271 ASN54	0	–	0	–	0	–	1^{E}	ILE290
DPP IV	2ONC	1	VAL121	0	–	0	–	3	PHE364 ALA306 TRP305	0	–	1	ASN272	3^{F}	GLY99 ASP96 LYS71
PTP-1B	2F70	0	–	0	–	1	LYS73	1	ARG199	0	–	0	–	2^{G}	PRO206 HIS208

Standard inhibitors or activator of pathways are: (A) miglitol, (B) metformin, (C) carbenoxolone, (D) thiadiazolidinone-8, (E) rosiglitazone, (F) sitagliptin and (G) ertiprotafib. Amino acids are: ALA, alanine; ARG, arginine; ASN, asparagine; ASP, aspartic acid; CYS, cysteine; GLN, glutamine; GLU, glutamic acid; GLY, glycine; HIS, histidine; ILE, isoleucine; LYS, lysine; MET, methionine; PHE, phenylalanine; PRO, proline; SER, serine; THR, threonine; TRP, tryptophan; TYR, tyrosine; VAL, valine.

TABLE 3 | Pi-Pi bonds (π-π bonds) formed by 4-ferrocenyl aniline (PFA), 1-(4-chlorobenzoyl)-3-(4-ferrocenylphenyl) urea (DPC1), 1-(3-chlorobenzoyl)-3-(4-ferrocenylphenyl) urea (DMC1), 1-(2-chlorobenzoyl)-3-(4-ferrocenylphenyl) urea (DOC1), bis (diphenylacetato) cadmium (II) (DPAA), bis (4-chlorophenylacetato) cadmium (II) (CPAA) and standard drugs against alpha amylase (AA), C-alpha glucosidase (C-AG), N-alpha glucosidase (N-AG), aldose reductase (AR), glucokinase (GK), glycogen phosphorylase (GP), fructose-1,6-bisphosphatase (FBP1), phosphoenolpyruvate carboxykinase (PEPCK), 11β-hydroxysteroid dehydrogenase-1 (11β-HSD1), glycogen synthase kinase-3β (GSK-3β), peroxisome proliferator-activated receptor γ (PPAR-γ), phosphatidylinositol 3 kinase (PI3K), phosphorylated-Akt (p-Akt), dipeptidyl peptidase-IV (DPP IV) and protein tyrosine phosphatase 1B (PTP-1B).

Proteins	PDB ID	PFA		DPC1		DMC1		DOC1		DPAA		CPAA		Standard drugs	
		π-π bonds	Amino acids	π-π bonds	Amino acids	π-π bonds	Amino acids	π-π bonds	Amino acids	π-π bonds	Amino acids	π-π bonds	Amino acids	π-π bonds	Amino acids
AA	2QMK	1	GLN302	1	PHE348	0	–	0	–	1	TRP316	0	–	0[A]	–
C-AG	3TON	0	–	0	–	0	–	0	–	0	–	0	–	0[A]	–
N-AG	2QMJ	2	GLY157 LYS48	0	–	0	–	0	–	0	–	0	–	0[A]	–
AR	1US0	2	ALA299 TRP111	2	TRP20 TRP111	2	TRP20 TRP111	3	TRP20 TRP111 PHE122	0	–	0	–	0[B]	–
GK	IV4S	0	–	1	SER64	0	–	0	–	1	HIS218	0	–	0[B]	–
GP	1L7X	0	–	0	–	0	–	0	–	0	–	0	–	0[B]	–
FBP1	2JJK	0	–	0	–	0	–	0	–	0	–	0	–	0[B]	–
PEPCK	1KHB	0	–	0	–	0	–	0	–	0	–	0	–	0[B]	–
11β-HSD1	2BEL	0	–	0	–	0	–	1	TYR183	1	TYR177	1	TYR177	0[C]	–
GSK-3β	1Q4L	0	–	0	–	0	–	0	–	0	–	0	–	0[D]	–
PPAR-γ	2PRG	0	–	0	–	0	–	0	–	0	–	0	–	0[E]	–
PI3K	1E7U	0	–	0	–	0	–	0	–	0	–	1	TYR608	0[E]	–
p-Akt	3O96	0	–	0	–	0	–	1	TRP80	0	–	1	TRP80	1[E]	TRP80
DPP IV	2ONC	0	–	0	–	0	–	0	–	1	TRP154	0	–	0[F]	–
PTP-1B	2F70	0	–	0	–	0	–	0	–	0	–	0	–	0[G]	–

Standard inhibitors or activator of pathways are: (A) miglitol, (B) metformin, (C) carbenoxolone, (D) thiadiazolidinone-8, (E) rosiglitazone, (F) sitagliptin, and (G) ertiprotafib. Amino acids are: ALA, alanine; GLN, glutamine; GLY, glycine; HIS, histidine; LYS, lysine; PHE, phenylalanine; SER, Serine; TRP, tryptophan; TYR, tyrosine.

control group were 578 ± 12.55, 560 ± 15.78, 586 ± 4.78, 572 ± 9.66, and 581 ± 7.94 mg/dL respectively. Blood glucose levels of DPAA (1 mg/Kg) treated group were 522 ± 19.70, 500 ± 24.59, 447 ± 17.48 ($P < 0.05$ vs. diabetic control), 470 ± 20.26 and 548 ± 29.25 mg/dL respectively. Blood glucose levels of DPAA (5 mg/Kg) treated group were 361 ± 60.93, 215 ± 65.25, 174 ± 47.36, 302 ± 28.13, and 318 ± 30.93 mg/dL ($P < 0.001$ vs. diabetic control) respectively. Blood glucose levels of DPAA (10 mg/Kg) treated group were 273 ± 37.69, 167 ± 40.54, 139 ± 31.11, 131 ± 30.78, and 102 ± 6.77 mg/dL ($P < 0.001$ vs. diabetic control) respectively. Blood glucose levels of metformin (500 mg/Kg) treated group were 534 ± 21.98, 460 ± 26.25, 429 ± 30.01 ($P < 0.01$ vs. diabetic control), 402 ± 32.67 and 391 ± 34.24 mg/dL ($P < 0.001$ vs. diabetic control) respectively (**Figure 5**). Blood glucose levels of DPC1 (1 mg/Kg) treated group were 600 ± 0.00, 560 ± 28.60, 409 ± 82.53, 395 ± 80.70, and 369 ± 76.86 mg/dL ($P < 0.05$ vs. diabetic control) respectively. Blood glucose levels of DPC1 (5 mg/Kg) treated group were 196 ± 21.91, 181 ± 17.08, 170 ± 18.25, 154 ± 24.03, and 119 ± 17.99 mg/dL ($P < 0.001$ vs. diabetic control) respectively. Blood glucose levels of DPC1 (10 mg/Kg) treated group were 204 ± 14.87 ($P < 0.001$ vs. diabetic control), 570 ± 29.20, 568 ± 31.60, 321 ± 86.36 ($P < 0.05$ vs. diabetic control), and 207 ± 61.84 mg/dL ($P < 0.001$ vs. diabetic control) respectively (**Figure 6**).

Effect on Body Weight

At 20th treatment day, body weight of DPAA 1, 5 and 10 mg/Kg treated groups were improved by +3.8, +3.5, and +2.3 g values respectively. Body weight of metformin (500 mg/Kg) treated group was reduced to −1.8 g at 20th treatment day (**Table 5**). At 20th treatment day, body weight of DPC1 1, 5, and 10 mg/Kg treated group changed by −1.0, +5.0, and −0.6 g values respectively (**Table 6**).

Effect on Glucose Tolerance

At 0, 30, 60, 90, and 120 min., blood glucose levels of non-diabetic control (saline, 10 mL/Kg) group were 266 ± 12.53, 204 ± 18.50, 168 ± 11.97, 145 ± 14.17, and 111 ± 6.68 mg/dL respectively. Blood glucose levels of alloxan (300 mg/Kg) treated diabetic control group were 457 ± 60.44, 473 ± 54.63, 402 ± 73.62, 376 ± 59.66, and 403 ± 66.36 mg/dL respectively. Blood glucose levels of DPAA (10 mg/Kg) treated group were 477 ± 28.40, 361 ± 50.34, 283 ± 48.48, 238 ± 46.97, and 193 ± 30.19 mg/dL ($P < 0.001$ vs. diabetic control) respectively. Blood glucose levels of metformin (500 mg/Kg) treated group were 275 ± 19.46, 246 ± 18.20 ($P < 0.01$ vs. diabetic control), 178 ± 32.80 ($P < 0.05$ vs. diabetic control), 147 ± 27.66 ($P < 0.01$ vs. diabetic control) and 113 ± 21.55 mg/dL ($P < 0.001$ vs. diabetic control) respectively (**Figure 7**). Blood glucose levels of DPC1 (5 mg/Kg) treated group were 317 ± 36.79, 205 ±

TABLE 4 | Hydrophobic interactions formed by 4-ferrocenyl aniline (PFA), 1-(4-chlorobenzoyl)-3-(4-ferrocenylphenyl) urea (DPC1), 1-(3-chlorobenzoyl)-3-(4-ferrocenylphenyl) urea (DMC1), 1-(2-chlorobenzoyl)-3-(4-ferrocenylphenyl) urea (DOC1), bis (diphenylacetato) cadmium (II) (DPAA), bis (4-chlorophenylacetato) cadmium (II) (CPAA) and standard drugs against alpha amylase (AA), C-alpha glucosidase (C-AG), N-alpha glucosidase (N-AG), aldose reductase (AR), glucokinase (GK), glycogen phosphorylase (GP), fructose-1,6-bisphosphatase (FBP1), phosphoenolpyruvate carboxykinase (PEPCK), 11β-hydroxysteroid dehydrogenase-1 (11β-HSD1), glycogen synthase kinase-3β (GSK-3β), peroxisome proliferator-activated receptor γ (PPAR-γ), phosphatidylinositol 3 kinase (PI3K), phosphorylated-Akt (p-Akt), dipeptidyl peptidase-IV (DPP IV) and protein tyrosine phosphatase 1B (PTP-1B).

Protein targets	PDB ID	Amino acid residues forming hydrophobic interactions						
		PFA	DPC1	DMC1	DOC1	DPAA	CPAA	Standard drugs
AA	2QMK	THR314	GLY304	TRP59	ASN352 GLY351	ASN352 PHE348 ARG346	GLU484 SER478	–[A]
C-AG	3TON	MET1778	ASN1776 LEU1740 1LE1801	VAL1809 SER1811 THR1810 VAL1812 SER1813 1LE1814	ASN1776 LEU1740 ILE1801 THR1810	ASN1776 VAL1812 THR1810 MET1778	VAL1807 VAL1809 ASN1776	–[A]
N-AG	2QMJ	SER155	VAL116 SER118 GLN117 PHE119 HIS115	LYS534 ALA285 LYS776	ILE523 PHE522 ALA285	LYS776 PHE535 ALA285 PRO287 LEU286	ALA537 ALA285 ASP777	ALA285[A]
AR	1US0	–	CYC298 TRP219	CYS298	CYS298 TRP79	TRP111 VAL47 TRP219	TYR48	–[B]
GK	IV4S	–	PRO66 TYR215 THR65	–	VAL455 PRO66 THR65	ILE211 VAL455 PRO66 THR65 TYR214 VAL455	PRO66 THR65 TYR214	ARG63[B]
GP	1L7X	GLY135	GLY135 LEU136 VAL455 ALA673 TYR573	HIS377 GLY135	GLY134 GLY135 LYS680 ARG569	GLY677 THR676 LEU136 ALA673 HIS377	ALA265	–[B]
FBP1	2JJK	–	SER46 ALA51	–	SER46 ALA51	ALA51 PRO188	ALA51 LYS72 LYS50	–[B]
PEPCK	1KHB	MN701 LYS290	THR339 ASN344 GLY338	ASN292 PRO337 THR339	ASN292 PHE530 THR343	PRO337 THR343 PHE530 VAL335 ASN292	PHE525 GLY289	ASN533 PHE525[B]
11β-HSD1	2BEL	ILE121	ALA226 THR124	THR222	THR124 ALA226	ALA223 VAL227 THR222 SER170	LEU171 THR124 ASN123 THR222	THR222 THR124 ASN123 TYR177[C]

(Continued)

TABLE 4 | Continued

Protein targets	PDB ID	Amino acid residues forming hydrophobic interactions						
		PFA	DPC1	DMC1	DOC1	DPAA	CPAA	Standard drugs
GSK-3β	1Q4L	–	LEU132	ASP200	LEU188	ASP90 GLN295 PRO294	ARG223 ILE228 SER215 ASN287	ASN64[D]
PPAR-γ	2PRG	–	CYS285	MET364	–	GLY284 LEU330	HIS449 CYS285	CYS285[E]
PI3K	1E7U	–	PHE497 THR1043 SER1044 LYS1045	ASN634 LYS591	PRO563 LEU564	TRP229 SER824 LEU823 GLU826 ASN825	TRP355 ALA528 ILE420	TRP355 ALA528[E]
p-Akt	3O96	VAL270 ILE290	–	GLN79	–	LEU264 TYR272	LEU264	THR291[E]
DPP IV	2ONC	–	–	–	–	THR156 ILE107	VAL279 SER277 THR280 TYR330	PHR98 PHE95 GLU97 ASP96[F]
PTP-1B	2F70	LYS73	LYS73 GLN78	LYS73 GLN78	GLY202	LYS73 GLN78 PRO206	GLN78 SER80 HIS60	GLN102 HIS208 PRO206[G]

Standard inhibitors or activator of pathways are: (A) miglitol (B) metformin, (C) carbenoxolone, (D) thiadiazolidinone-8, (E) rosiglitazone, (F) sitagliptin and (G) ertiprotafib. Amino acids are: ALA, alanine; ARG, arginine; ASN, asparagine; ASP, aspartic acid; CYS, cysteine; GLN, glutamine; GLU, glutamic acid; GLY, glycine; HIS, histidine; ILE, isoleucine; LYS, lysine; MET, methionine; PHE, phenylalanine; PRO, proline; SER, serine; THR, threonine; TRP, tryptophan; TYR, tyrosine; VAL, valine.

23.35, 138 ± 8.12, 100 ± 9.69, and 87 ± 4.97 mg/dL, with significance level of $P < 0.001$ vs. diabetic control at 30, 90, and 120 min., while $P < 0.01$ vs. diabetic control at 60 min (**Figure 8**).

Effect on HbA1C

HbA1C value of non-diabetic control (saline, 10 mL/Kg) group was 3.1%. DPAA and DPC1 (1, 5, and 10 mg/Kg) treated group showed significant ($P < 0.001$ vs. diabetic control group) reduction in the HbA1C levels in alloxan-induced diabetic animals. Metformin (500 mg/Kg) treated showed reduction in HbA1C levels having $P < 0.001$ compared to the diabetic control group (**Table 7**).

Acute Toxicity

DPAA at doses of 15, 25, 50, and 100 mg/Kg caused 40, 80, and 100% mortality respectively. DPC1 at tested doses of 25, 50, and 100 mg/Kg did not exhibit any mortality (**Table 8**).

DISCUSSION

The application of computational approaches has turn out to be vital constituent of drug discovery strategy processes and ligand/structure based virtual screening is extensively used for this purpose (Langer and Hoffmann, 2001; Bajorath, 2002). From 1980s, molecular docking was found to be a key method of structure based virtual screening and it is still a very active area in research (Kuntz et al., 1982; Gohlke and Klebe, 2002; Kitchen et al., 2004). Virtual screening carried out through molecular docking that has become essential for quick and cost effective screening of the ligands on basis of structures (de Lange et al., 2014; Zhong et al., 2015). Patch dock server used in the study, assess ligand-protein complex by scoring on basis of appropriate geometry and atomic desolvation free energy (Schneidman-Duhovny et al., 2005). Lower ACE value indicates lower desolvation energy which is favorable for ligand-protein complex (Guo et al., 2012). In stated cases, strength of π-π interaction for stabilization of structural complex is comparable to the strength of hydrogen bonding (Blakaj et al., 2001). In ground state, loss of π-π interaction does not lead to affect the active-site conformation but results in 20–30 times reduction in the rate constant of chemical activity (Pecsi et al., 2010). Hydrophobic interactions can also enhance affinity of ligand against target protein (Patil et al., 2010). Evaluation of binding affinity between ligands and proteins complexes was done by assessing ACE value, H-bonds, π-π interaction and hydrophobic interactions.

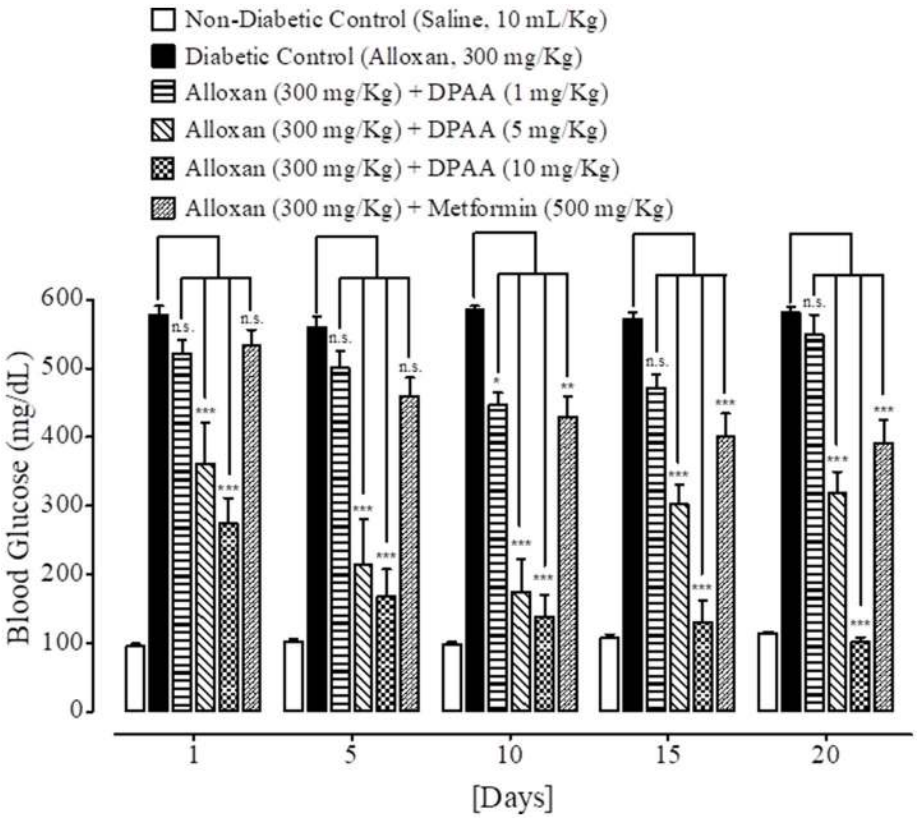

FIGURE 5 | Bar-graph representing blood glucose levels at different treatment days of saline treated group (non-diabetic control), alloxan treated group (diabetic control), inhibitory effect of bis (diphenylacetato) cadmium (II) (DPAA) at different doses (1–10 mg/Kg) and metformin treated group against alloxan-induced hyperglycemia in mice. Data presented as mean ± SEM. Statistical analysis used one-way ANOVA, followed by *post-hoc* Tukey's test. $^{*}P < 0.05$, $^{**}P < 0.01$, $^{***}P < 0.001$ comparison of the blood glucose levels of DPAA and metformin treated groups vs. diabetic control group. n.s., non-significant. The sample size in each group comprised of five mice ($n = 5$).

We have found in this study, DPAA showed best binding score with lowest ACE value against GK and most of the target proteins than standard and other test compounds. We can anticipate that it has highest binding affinity against GK. The ligands order of affinity against GK was found as; DPAA > DPC1 > DMC1 > DOC1 > CPAA > PFA > metformin. The ligands order of affinity against AR was shown as; DOC1 > DPC1 > DPAA > DMC1 > CPAA > PFA > metformin. Test compounds that are high in order formed π-π bonds, hydrophobic bonds and H-bonds with GK and AR, while metformin and miglitol showed only H-bonding. Moreover all ligands interact with allosteric binding site of GK (Matschinsky et al., 2006; Min et al., 2017) and AR (Antony and Vijayan, 2015). The ligands order of affinity against AA was found as; DPAA > DPC1 > DMC1 > DOC1 > CPAA > PFA > miglitol. Compounds with high affinity did not show binding with TRP59, ASP197, and GLU233 which are reported as essential amino acid residue of AA (Piparo et al., 2008). Only DMC1 showed interaction against TRP59, but do not show highest binding affinity. The ligands order of affinity against FBP1 was shown as; DPAA > DMC1 > DOC1 > DPC1 > PFA > metformin > CPAA. Along with H-bonds and hydrophobic interactions, other interactions such as alky, π-alky and van der waals interactions are shown by test compounds with high affinity. Amino acids; PRO188, ARG49, ALA51, ALA189, and PRO100 are found to be important. The ligands order of affinity against PEPCK was found as; DMC1 > DPAA > DOC1 > DPC1 > CPAA > PFA > metformin. All ligands exhibited interactions with reported binding site of PEPCK (Katiyar et al., 2015). Moreover, H-bonding is found to be important for ligand-PEPCK complex.

The ligands order of affinity against GP was found as; DOC1 > DPAA > DMC1 > DPC1 > CPAA > metformin > PFA. DOC1, DPAA, and DMC1 showed interactions with ASP283, a conservative amino acid (Hudson et al., 1993) and ARG569 that is responsible for salt bridge interactions (Barford and Johnson, 1989). The ligands order of affinity against N-AG was found as; DPAA > 1 > DMC1 > DPC1 > CPAA > PFA > miglitol. Ligands are not involved in making any strong bonding with reported binding site (Saqib and Siddiqi, 2008). The ligands order of affinity against C-AG was found as; DPAA > DPC1 > DOC1 > DMC1 > CPAA > PFA > miglitol. H-bonds and hydrophobic interactions are found to be important, but ligands did not show bonding with stated binding site (Ren et al., 2011). Amino acid ASN1776 is found to be vital. The ligands order

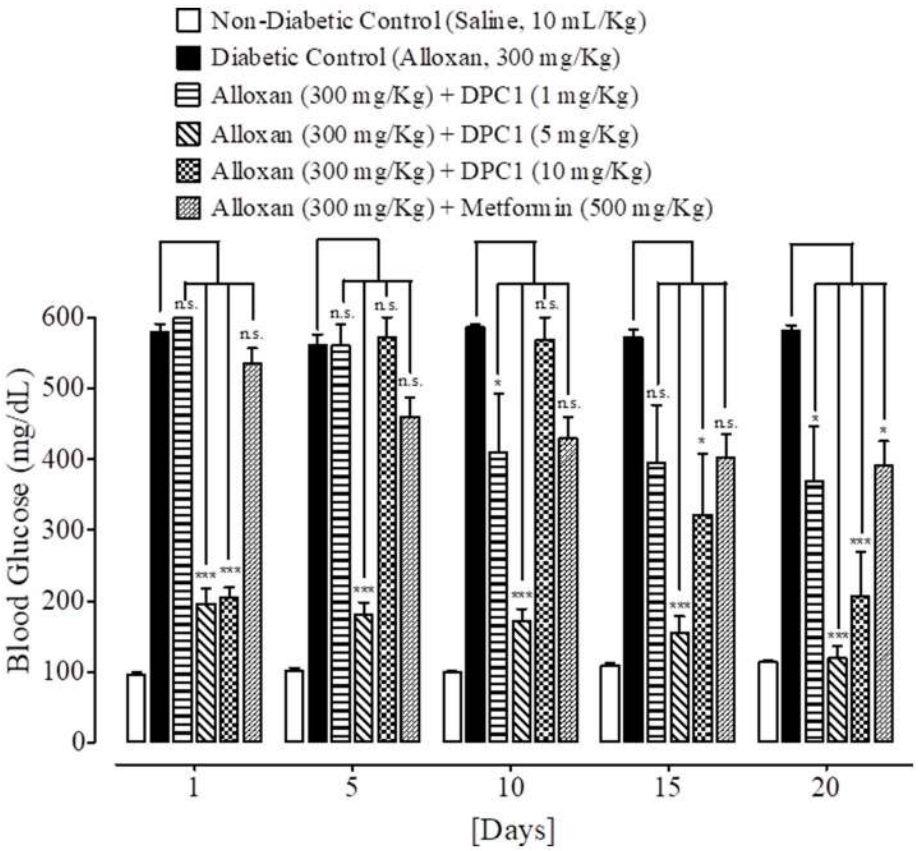

FIGURE 6 | Bar-graph representing blood glucose levels at different treatment days of saline treated group (non-diabetic control), alloxan treated group (diabetic control), inhibitory effect of 1-(4-chlorobenzoyl)-3-(4-ferrocenylphenyl) urea (DPC1) at different doses (1–10 mg/Kg) and metformin treated group against alloxan-induced hyperglycemia in mice. Data presented as mean ± SEM. Statistical analysis used one-way ANOVA, followed by *post-hoc* Tukey's test. $^{*}P < 0.05$, $^{***}P < 0.001$ comparison of the blood glucose levels of DPC1 and metformin treated groups vs. diabetic control group. n.s., non-significant. The sample size in each group comprised of five mice ($n = 5$).

of affinity against GSK-3β was found as; DPAA > DPC1 > DOC1 > DMC1 > CPAA > TDZD-8 > PFA. All ferrocene derivatives showed interactions with CYS199 which is reported as important amino acid of binding site (Perez et al., 2011). DPAA lack interaction with CYS199, but still exhibited high binding affinity.

The ligands order of affinity against 11β-HSD1 was found as; carbenoxolone > DPAA > DPC1 > DMC1 > DOC1 > CPAA > PFA. Carbenoxolone, DPAA and DPC1 exhibited high affinity and formed interactions with TYR177 which is reported as key amino acid (Kim et al., 2006). The ligands order of affinity against p-Akt was found as; DPAA > DOC1 > rosiglitazone > DMC1 > DPC1 > PFA > CPAA. Ligands having high binding affinity formed interactions with TYR272 and VAL270. The ligands order of affinity against PI3K was found as; rosiglitazone > DPAA > CPAA > DOC1 > DPC1 > DMC1 > PFA. It is revealed that homoleptic cadmium carboxylates showed more affinity than ferrocene incorporated acyl ureas. The ligands order of affinity against PPAR-γ was found as; DPAA > rosiglitazone > DPC1 > DMC1 > DOC1 > CPAA > PFA. Ligand with high affinity showed hydrophobic interactions. All ligands showed interaction with ARG288, an essential amino acid of binding site (Choi et al., 2010). The ligands order of affinity against DPP IV was found as; DOC1 > DMC1 > DPC1 > DPAA > CPAA > sitagliptin > PFA. DOC1, DMC1 and DPC1 showed different interactions with HIS363, LEU410, and ALA409. These amino acid residues are found to be crucial against DPP IV. The ligands order of affinity against PTP-1B was found as; ertiprotafib > DPAA > DMC1 > DPC1 > CPAA > PFA > DOC1. Ligands showed interactions with amino acid PRO206. Ligands having high affinity showed H-bonds and hydrophobic interactions against PRO206. Interaction with amino acids of reported binding site was not shown by any ligand (Jin et al., 2016).

In current study, only enzymes are targeted that are involved in activation or inhibition of pathways important for pathogenesis of diabetes. By using molecular docking technique, ligands can be tested against other possible anti-diabetic targets such as sulfonylurea receptors, GLUT 1, GLUT 2, and GLUT 4 receptors as well as ion channels such as involvement of calcium channels, ligand gated K^+ channels and Na^+/K^+ transporters. In result of virtual screening, DPAA and DPC1 are found to be potential agonists of GK. GK activating effect can be a

TABLE 5 | Effect of bis (diphenylacetato) cadmium (II) (DPAA) and metformin at different treatment days on body weight (g) of alloxan-induced diabetic mice.

Treatment	Day 1	Day 5	Day 10	Day 15	Day 20
Alloxan (300 mg/Kg) + DPAA (1 mg/Kg)	29.0 ± 2.09	30.5 ± 1.78	31.0 ± 1.54	32.4 ± 1.66	32.8 ± 1.62
Alloxan (300 mg/Kg) + DPAA (5 mg/Kg)	32.3 ± 1.07	33.0 ± 1.29	34.3 ± 1.25	35.3 ± 1.36	35.8 ± 1.36
Alloxan (300 mg/Kg) + DPAA (10 mg/Kg)	34.9 ± 0.85	35.8 ± 0.31	36.5 ± 0.70	36.9 ± 0.82	37.2 ± 0.89
Alloxan (300 mg/Kg) + Metformin (500 mg/Kg)	23.3 ± 1.22	22.7 ± 1.32	22.3 ± 1.33	21.7 ± 1.34	21.5 ± 1.35

Data presented as mean ± SEM. The sample size in each group comprised of five animals (n = 5).

TABLE 6 | Effect of 1-(4-chlorobenzoyl)-3-(4-ferrocenylphenyl) urea (DPC1) at different treatment days on body weight (g) of alloxan-induced diabetic mice.

Treatment	Day 1	Day 5	Day 10	Day 15	Day 20
Alloxan (300 mg/Kg) + DPC1 (1 mg/Kg)	32.9 ± 0.79	31.0 ± 1.48	29.9 ± 1.51	29.9 ± 1.36	31.9 ± 1.20
Alloxan (300 mg/Kg) + DPC1 (5 mg/Kg)	30.3 ± 1.94	30.0 ± 0.87	29.4 ± 0.89	32.9 ± 1.48	35.3 ± 1.27
Alloxan (300 mg/Kg) + DPC1 (10 mg/Kg)	34.5 ± 0.47	31.3 ± 1.00	30.4 ± 0.43	31.6 ± 1.34	33.9 ± 0.53

Data presented as mean ± SEM. The sample size in each group comprised of five animals (n = 5).

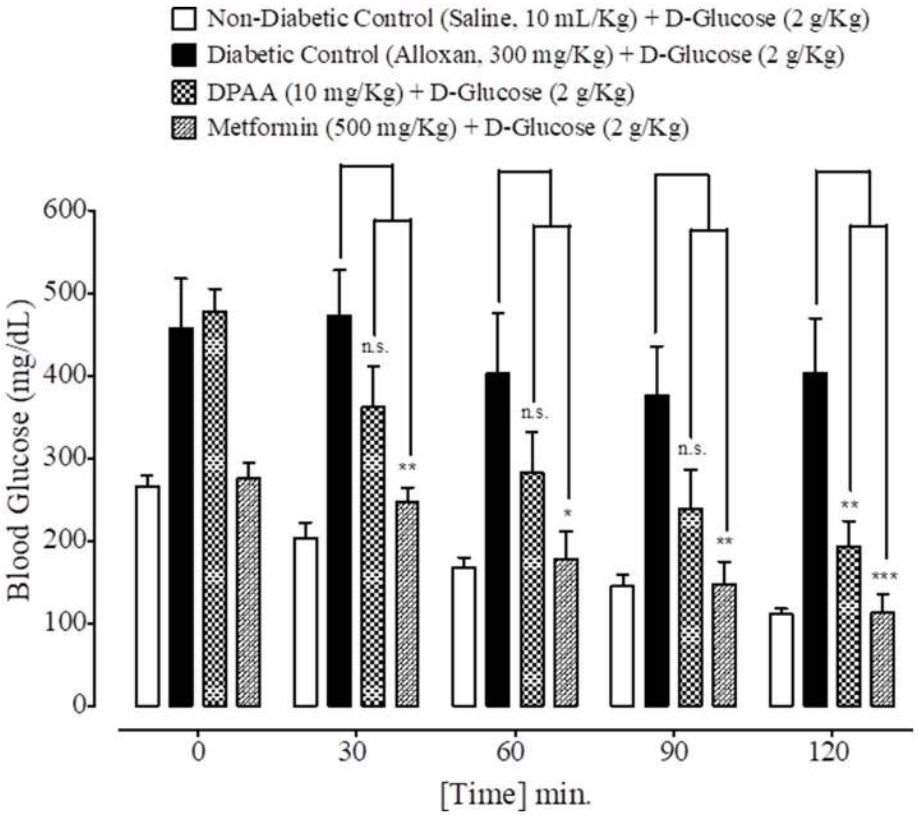

FIGURE 7 | Bar graph representing blood glucose levels at different time intervals (0–120 min.) after administration of oral glucose load in mice of saline treated group (non-diabetic control), alloxan treated group (diabetic control), bis (diphenylacetato) cadmium (II) (DPAA) treated group and metformin pre-treated group. Data expressed as mean ± SEM. Statistical analysis used one-way ANOVA, followed by *post-hoc* Tukey's test. *$P < 0.05$, **$P < 0.01$, ***$P < 0.001$ comparison of the blood glucose levels of DPAA and metformin treated group vs. diabetic control group. n.s., non-significant. The sample size in each group comprised of five mice ($n = 5$).

proposed mechanism for anti-diabetic effect. Alloxan-induced diabetes model was used to validate the GK activating effect of DPAA and DPC1. It has been reported that GK activity was found to be same in alloxan- and streptozotocin-induced diabetes by depletion of β-cells as in control group (Matschinsky, 2009).

DPAA and DPC1 (1 mg/Kg) exhibited results like diabetic control group, so dose <1 mg/Kg cannot be used for significant

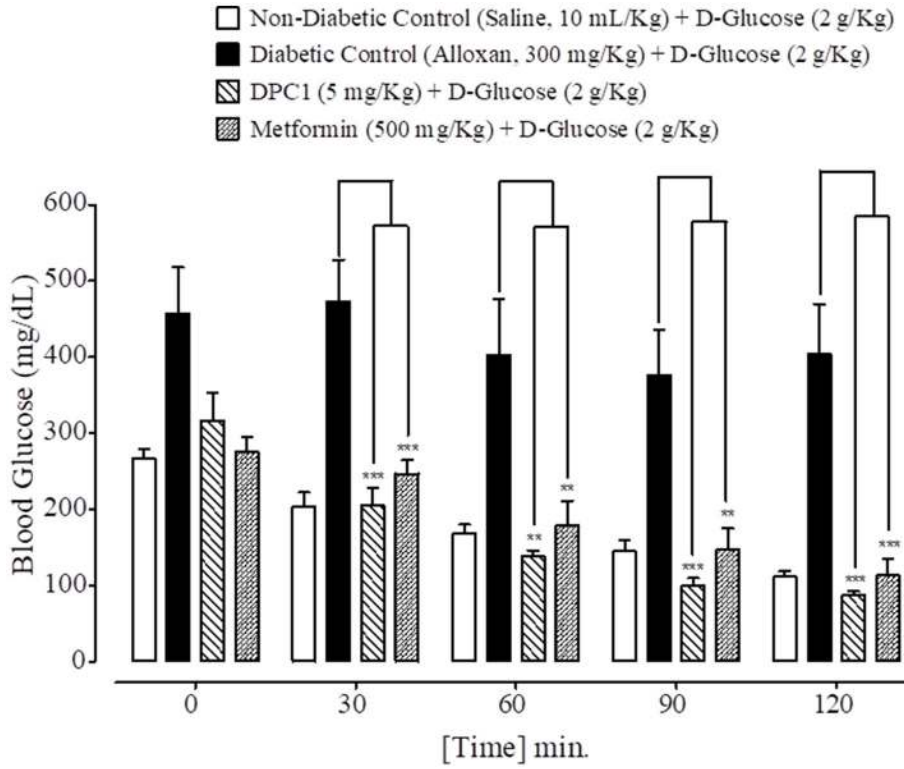

FIGURE 8 | Bar graph representing blood glucose levels at different time intervals (0–120 min.) after administration of oral glucose load in mice of saline treated group (non-diabetic control), alloxan treated group (diabetic control), 1-(4-chlorobenzoyl)-3-(4-ferrocenylphenyl) urea (DPC1) treated group and metformin treated group. Data expressed as mean ± SEM. Statistical analysis used one-way ANOVA, followed by *post-hoc* Tukey's test. $^{**}P < 0.01$, $^{***}P < 0.001$ comparison of the blood glucose levels of DPC1 and metformin treated group vs. diabetic control group. The sample size in each group comprised of five mice ($n = 5$).

TABLE 7 | Effect of bis (diphenylacetato) cadmium (II) (DPAA), 1-(4-chlorobenzoyl)-3-(4-ferrocenylphenyl) urea (DPC1) and metformin on glycosylated hemoglobin A1C (HbA1C) in mice.

Groups	HbA1C Levels (%)
Non-Diabetic Control (Saline, 10 mL/Kg)	3.1 ± 0.05
Diabetic Control (Alloxan, 300 mg/Kg)	6.6 ± 0.11
Alloxan (300 mg/Kg) + DPAA (1 mg/Kg)	4.4 ± 0.10***
Alloxan (300 mg/Kg) + DPAA (5 mg/Kg)	3.6 ± 0.06***
Alloxan (300 mg/Kg) + DPAA (10 mg/Kg)	3.3 ± 0.12***
Alloxan (300 mg/Kg) + DPC1 (1 mg/Kg)	4.2 ± 0.07***
Alloxan (300 mg/Kg) + DPC1 (5 mg/Kg)	3.9 ± 0.05***
Alloxan (300 mg/Kg) + DPC1 (10 mg/Kg)	3.7 ± 0.18***
Alloxan (300 mg/Kg) + Metformin (500 mg/Kg)	3.4 ± 0.09***

*Data expressed as mean ± SEM. Statistical analysis used one-way ANOVA, followed by post-hoc Tukey's test. ***P < 0.001 comparison of the HbA1C levels of DPAA, DPC1 and metformin treated groups vs. diabetic control group. The sample size in each group comprised of five mice (n = 5).*

TABLE 8 | Percentage (%age) mortality of mice caused by bis (diphenylacetato) cadmium (II) (DPAA) and 1-(4-chlorobenzoyl)-3-(4-ferrocenylphenyl) urea (DPC1) at different doses.

Test Compounds	Dose (mg/Kg)	Mortality (%)
DPAA	15	40
	25	80
	50	100
	100	100
DPC1	25	0
	50	0
	100	0

Mortality (%) = (No. of dead mice/Total No. of mice in group) × 100. The sample size in each group comprised of five mice (n = 5).

anti-diabetic activity. DPAA (5 and 10 mg/Kg) and DPC1 (5 mg/Kg) showed time-dependent hypoglycemic effect than metformin. DPC1 (10 mg/Kg) produced abrupt increase in glucose levels at day 5 and 10th. Normally 1–2 mg of iron circulates in the blood (Andrews, 1999). Iron overload can lead to insulin resistance and impaired glucose utilization. Enhanced insulin sensitivity and glucose utilization has been reported in iron-deficient rats than iron-sufficient control group (Henderson et al., 1986; Borel et al., 1993). This effect can also be resulted by catalysis of highly reactive OH· radicals formation by iron via Fenton reaction (Crichton et al., 2002). DPC1 dose ≥10 mg/kg can reverse the hypoglycemic effect, while toxicity test revealed 10 mg/Kg as highest safest dose of DPAA.

DPAA and DPC1 reversed the reduced body weight compared to metformin. Both compounds enhanced the oral glucose tolerance as caused by metformin. Compounds produced dose-dependent effect in reducing HbA1C levels and found to be effective as long term anti-diabetic agent (Koenig et al., 1976). Enhanced hypoglycemic effect of DPAA could be due to the reduction of plasma selenium levels by cadmium moiety (Gümüşlü et al., 1997; Bleys et al., 2007) along with α-glucosidase inhibition by carboxylate group (Roy et al., 2015). Higher effect of DPC1 could be possible by GP inhibition due to acyl urea group (Klabunde et al., 2005). Antioxidant effect of DPC1 could also be the proposed mechanism for anti-diabetic activity (Asghar et al., 2015).

CONCLUSIONS

Computational studies reveal binding affinities of selected ferrocene-based acyl ureas (PFA, DPC1, DMC1, and DOC1) and homoleptic cadmium carboxylates (DPAA and CPAA) against different proteins targets involved in pathogenesis of DM. Highest affinity was exhibited by DPAA and DPC1 against glucokinase. *In vivo* assays also validated the anti-diabetic effect of DPAA and DPC1. Both of the test compounds enhanced the glucose tolerance and decrease the HbA1C levels.

AUTHOR CONTRIBUTIONS

SB carried out the computational studies, *in vivo* experimentations, evaluation of results and documentation. AK supervised the research project and drafted the final manuscript. FA and AB provided ferrocene derivatives. MU and SA provided the cadmium carboxylates. All authors read and approved the final manuscript.

ACKNOWLEDGMENTS

Authors are thankful to Ms. Hira Shahid, Department of Statistics, Quaid-e-Azam University Islamabad, for providing technical support in usage of softwares, evaluation of results and confirmation of statistics applied. We are also grateful to Riphah Academy of Research and Education (RARE), Riphah International University and Cantt Laboratory and Medical Imaging, for facilitation and support.

SUPPLEMENTARY MATERIAL

The Supplementary Material for this article can be found online at: https://www.frontiersin.org/articles/10.3389/fphar.2017.01001/full#supplementary-material

REFERENCES

Anderson, R. A., Cheng, N., Bryden, N. A., Polansky, M. M., Cheng, N., Chi, J., et al. (1997). Elevated intakes of supplemental chromium improve glucose and insulin variables in individuals with type 2 diabetes. *Diabetes* 46, 1786–1791. doi: 10.2337/diab.46.11.1786

Andrews, N. C. (1999). Disorders of iron metabolism. *New Eng. J. Med.* 341, 1986–1995. doi: 10.1056/NEJM199912233412607

Antony, P., and Vijayan, R. (2015). Identification of novel aldose reductase inhibitors from spices: a molecular docking and simulation study. *PLoS ONE* 10:e0138186. doi: 10.1371/journal.pone.0138186

Asgary, S., Parkhideh, S., Solhpour, A., Madani, H., Mahzouni, P., and Rahimi, P. (2008). Effect of ethanolic extract of Juglans *regia* L. on blood sugar in diabetes-induced rats. *J. Med. Food* 11, 533–538. doi: 10.1089/jmf.2007.0611

Asghar, F., Badshah, A., Hussain, R. A., Sohail, M., Akbar, K., and Butler, I. S. (2015). Synthesis, structural characterization, DNA binding and antioxidant potency of new ferrocene incorporated acyl ureas. *J. Organomet. Chem.* 797, 131–139. doi: 10.1016/j.jorganchem.2015.08.010

Asghar, F., Badshah, A., Lal, B., Zubair, S., Fatima, S., and Butler, I. (2017). Facile synthesis of fluoro, methoxy, and methyl substituted ferrocene-based urea complexes as potential therapeutic agents. *Bioorg. Chem.* 72, 215–227. doi: 10.1016/j.bioorg.2017.04.016

Bajorath, J. (2002). Integration of virtual and high-throughput screening. *Nat. Rev. Drug Discov.* 1, 882–894. doi: 10.1038/nrd941

Barberà, A., Gomis, R., Prats, N., Rodríguez-Gil, J., Domingo, M., Gomis, R., et al. (2001). Tungstate is an effective antidiabetic agent in streptozotocin-induced diabetic rats: a long-term study. *Diabetologia* 44, 507–513. doi: 10.1007/s001250100479

Barford, D., and Johnson, L. (1989). The allosteric transition of glycogen phosphorylase. *Nature* 340, 609–616. doi: 10.1038/340609a0

Blakaj, D. M., McConnell, K. J., Beveridge, D. L., and Baranger, A. M. (2001). Molecular dynamics and thermodynamics of protein– rna interactions: mutation of a conserved aromatic residue modifies stacking interactions and structural adaptation in the U1A– stem loop 2 RNA complex. *J. Am. Chem. Soc.* 123, 2548–2551. doi: 10.1021/ja005538j

Bleys, J., Navas-Acien, A., and Guallar, E. (2007). Serum selenium and diabetes in US adults. *Diabetes Care* 30, 829–834. doi: 10.2337/dc06-1726

Borel, M. J., Beard, J. L., and Farrell, P. A. (1993). Hepatic glucose production and insulin sensitivity and responsiveness in iron-deficient anemic rats. *Am. J. Phys. Endo. Met.* 264, E380–E390. doi: 10.1152/ajpendo.1993.264.3.E380

Bukhari, S. S., Abbasi, M. H., and Khan, M. A. (2015). Dose optimization of Alloxan for diabetes in albino mice. *Biologica (Pakistan)* 61, 301–305.

Chen, J., Dong, X., Zhao, J., and Tang, G. (2009). *In vivo* acute toxicity of titanium dioxide nanoparticles to mice after intraperitioneal injection. *J. Appl. Toxicol.* 29, 330–337. doi: 10.1002/jat.1414

Choi, J., Park, Y., Lee, H. S., Yang, Y., and Yoon, S. (2010). 1, 3-Diphenyl-1H-pyrazole derivatives as a new series of potent PPARγ partial agonists. *Bioorg. Med. Chem.* 18, 8315–8323. doi: 10.1016/j.bmc.2010.09.068

Crichton, R. R., Wilmet, S., Legssyer, R., and Ward, R. J. (2002). Molecular and cellular mechanisms of iron homeostasis and toxicity in mammalian cells. *J. Inorg. Biochem.* 91, 9–18. doi: 10.1016/S0162-0134(02)00461-0

de Lange, O., Wolf, C., Dietze, J., Elsaesser, J., Morbitzer, R., and Lahaye, T. (2014). Programmable DNA-binding proteins from Burkholderia provide a fresh perspective on the TALE-like repeat domain. *Nucl. Acids Res.* 42, 7436–7449. doi: 10.1093/nar/gku329

Doeing, D. C., Borowicz, J. L., and Crockett, E. T. (2003). Gender dimorphism in differential peripheral blood leukocyte counts in mice using cardiac, tail, foot, and saphenous vein puncture methods. *BMC Clin. Pathol.* 3:3. doi: 10.1186/1472-6890-3-3

Duhovny, D., Nussinov, R., and Wolfson, H. J. (2002). Efficient unbound docking of rigid molecules. *Lecture Notes Comput. Sci.* 2452, 185–200. doi: 10.1007/3-540-45784-4_14

Dunn, J. S., and McLetchie, N. (1943). Experimental alloxan diabetes in the rat. *Lancet* 242, 384–387. doi: 10.1016/S0140-6736(00)87397-3

Gohlke, H., and Klebe, G. (2002). Approaches to the description and prediction of the binding affinity of small-molecule ligands to macromolecular receptors. *Angew. Chem. Int. Ed.* 41, 2644–2676. doi: 10.1002/1521-3773(20020802)41:15<2644::AID-ANIE2644>3.0.CO;2-O

Gümüşlü, S., Yargiçoglu, P., Agar, A., Edremitlioglu, M., and Alicigüzel, Y. (1997). Effect of cadmium on antioxidant status in alloxane-induced diabetic rats. *Biol. Trace Elem. Res.* 57, 105–114. doi: 10.1007/BF02778193

Guo, F., Li, S. C., Wang, L., and Zhu, D. (2012). Protein-protein binding site identification by enumerating the configurations. *BMC Bioinformatics* 13:158. doi: 10.1186/1471-2105-13-158

Henderson, S. A., Dallman, P. R., and Brooks, G. A. (1986). Glucose turnover and oxidation are increased in the iron-deficient anemic rat. *Am. J. Physiol.* 250, E414–E421. doi: 10.1152/ajpendo.1986.250.4.E414

Heyliger, C. E., Tahiliani, A. G., and McNeill, J. H. (1985). Effect of vanadate on elevated blood glucose and depressed cardiac performance of diabetic rats. *Science* 227, 1474–1477. doi: 10.1126/science.3156405

Hu, F. B. (2011). Globalization of diabetes. *Diabetes Care* 34, 1249–1257. doi: 10.2337/dc11-0442

Hudson, J. W., Golding, G. B., and Crerar, M. M. (1993). Evolution of allosteric control in glycogen phosphorylase. *J. Mol. Biol.* 234, 700–721. doi: 10.1006/jmbi.1993.1621

Jin, T., Yu, H., and Huang, X.-F. (2016). Selective binding modes and allosteric inhibitory effects of lupane triterpenes on protein tyrosine phosphatase 1B. *Sci. Rep.* 6:20766. doi: 10.1038/srep20766

Katiyar, S. P., Jain, A., Dhanjal, J. K., and Sundar, D. (2015). Mixed inhibition of cPEPCK by genistein, using an extended binding site located adjacent to its catalytic cleft. *PLoS ONE* 10:e0141987. doi: 10.1371/journal.pone.0141987

Kim, K. W., Wang, Z., Busby, J., Tsuruda, T., Chen, M., Hale, C., et al. (2006). The role of tyrosine 177 in human 11β-hydroxysteroid dehydrogenase type 1 in substrate and inhibitor binding: an unlikely hydrogen bond donor for the substrate. *Biochim. Biophys. Acta* 1764, 824–830. doi: 10.1016/j.bbapap.2006.02.008

Kitchen, D. B., Decornez, H., Furr, J. R., Bajorath, J. (2004). Docking and scoring in virtual screening for drug discovery: methods and applications. *Nat. Rev.* 3, 935–949. doi: 10.1038/nrd1549

Klabunde, T., Wendt, K. U., Kadereit, D., Brachvogel, V., Burger, H.-J., Herling, A. W., et al. (2005). Acyl ureas as human liver glycogen phosphorylase inhibitors for the treatment of type 2 diabetes. *J. Med. Chem.* 48, 6178–6193. doi: 10.1021/jm049034y

Koenig, R. J., Peterson, C. M., Jones, R. L., Saudek, C., Lehrman, M., and Cerami, A. (1976). Correlation of glucose regulation and hemoglobin AIc in diabetes mellitus. *N. Engl. J. Med.* 295, 417–420. doi: 10.1056/NEJM197608192950804

Kuntz, I. D., Blaney, J. M., Oatley, S. J., Langridge, R., and Ferrin, T. E. (1982). A geometric approach to macromolecule–ligand interactions. *J. Mol. Biol.* 161, 269–288. doi: 10.1016/0022-2836(82)90153-X

Lal, B., Badshah, A., Altaf, A. A., Khan, N., and Ullah, S. (2011). Miscellaneous applications of ferrocene-based peptides/amides. *Appl. Org. Chem.* 25, 843–855. doi: 10.1002/aoc.1843

Langer, T., and Hoffmann, R. D. (2001). Virtual screening: an effective tool for lead structure discovery. *Curr. Pharm. Design* 7, 509–527. doi: 10.2174/1381612013397861

Marguet, D., Baggio, L., Kobayashi, T., Bernard, A.M., Pierres, M., and Nielsen, P. F. (2000). Enhanced insulin secretion and improved glucose tolerance in mice lacking CD26. *Proc. Natl. Acad. Sci. U.S.A.* 97, 6874–6879. doi: 10.1073/pnas.120069197

Mathers, C. D., and Loncar, D. (2006). Projections of global mortality and burden of disease from 2002 to 2030. *PLoS Med.* 3:e442. doi: 10.1371/journal.pmed.0030442

Matschinsky, F. M. (2009). Assessing the potential of glucokinase activators in diabetes therapy. *Nat. Rev. Drug Discov.* 8, 399–416. doi: 10.1038/nrd2850

Matschinsky, F. M., Magnuson, M. A., Zelent, D., Jetton, T. L., Doliba, N., Han, Y., et al. (2006). The network of glucokinase-expressing cells in glucose homeostasis and the potential of glucokinase activators for diabetes therapy. *Diabetes* 55, 1–12. doi: 10.2337/diabetes.55.01.06.db05-0926

Min, Q., Cai, X., and Sun, W. (2017). Identification of mangiferin as a potential Glucokinase activator by structure-based virtual ligand screening. *Sci. Rep.* 7:44681. doi: 10.1038/srep44681

Nathan, D. M., Buse, J. B., Davidson, M. B., Ferrannini, E., Holman, R. R., Sherwin, R., et al. (2009). Medical management of hyperglycemia in type 2 diabetes: a consensus algorithm for the initiation and adjustment of therapy. *Diabetes Care* 32, 193–203. doi: 10.2337/dc08-9025

Ozcelikay, A. T., Becker, D. J., Ongemba, L. N., Pottier, A. M., Henquin, J. C., and Brichard, S. M. (1996). Improvement of glucose and lipid metabolism in diabetic rats treated with molybdate. *Am. J. Phys. Endo. Met.* 270, E344–E352. doi: 10.1152/ajpendo.1996.270.2.E344

Pecsi, I., Leveles, I., Harmat, V., Vertessy, B. G., and Toth, J. (2010). Aromatic stacking between nucleobase and enzyme promotes phosphate ester hydrolysis in dUTPase. *Nucl. Acids Res.* 38, 7179–7186. doi: 10.1093/nar/gkq584

Perez, D. I., Palomo, V., Pérez, C., Gil, C., Dans, P. D., Luque, F. J., et al. (2011). Switching reversibility to irreversibility in glycogen synthase kinase 3 inhibitors: clues for specific design of new compounds. *J. Med. Chem.* 54, 4042–4056. doi: 10.1021/jm1016279

Piparo, E, L., Scheib, H., Frei, N., Williamson, G., Grigorov, M., and Chou, C. J. (2008). Flavonoids for controlling starch digestion: structural requirements for inhibiting human α-amylase. *J. Med. Chem.* 51, 3555–3561. doi: 10.1021/jm800115x

Ren, L., Qin, X., Cao, X., Wang, L., Bai, F., Bai, G., et al. (2011). Structural insight into substrate specificity of human intestinal maltase-glucoamylase. *Protein Cell* 2, 827–836. doi: 10.1007/s13238-011-1105-3

Patil, R., Das, S., Stanley, A., Yadav, L., Sudhakar, A., and Varma, A. K. (2010). Optimized hydrophobic interactions and hydrogen bonding at the target-ligand interface leads the pathways of drug-designing. *PLoS ONE* 5:e12029. doi: 10.1371/journal.pone.0012029

Roy, M., Devi, S. S., Roy, S., Singh, C., and Singh, K. S. (2015). Synthesis, characterization, crystal structures and *in vitro* antimicrobial activities of triorganotin (IV) complexes of azo-dicarboxylates. *Inorg. Chim. Acta* 426, 89–98. doi: 10.1016/j.ica.2014.11.030

Saqib, U., and Siddiqi, M. (2008). Probing ligand binding interactions of human alpha glucosidase by homology modeling and molecular docking. *Intern. J. Integr. Biol.* 2, 116–121.

Saudek, C. D., Herman, W. H., Sacks, D. B., Bergenstal, R. M., Edelman, D., and Davidson, M. B. (2008). A new look at screening and diagnosing diabetes mellitus. *J. Clin. Endocrinol. Met.* 93, 2447–2453. doi: 10.1210/jc.2007-2174

Schneidman-Duhovny, D., Inbar, Y., Nussinov, R., and Wolfson, H. J. (2005). PatchDock and SymmDock: servers for rigid and symmetric docking. *Nucl. Acids Res.* 33, W363–W367. doi: 10.1093/nar/gki481

Siva, L., and Kumar, V. S. (2013). Role of iron and copper in diabetics. *Bull. Pharm. Med. Sci.* 1, 210–221.

Sussman, J. L., Lin, D., Jiang, J., Manning, N. O., Prilusky, J., Ritter, O., et al. (1998). Protein Data Bank (PDB): database of three-dimensional structural information of biological macromolecules. *Acta Cryst. Sect. D Biol. Crystallogr.* 54, 1078–1084. doi: 10.1107/S0907444998009378

Tuomi, T. (2005). Type 1 and type 2 diabetes. *Diabetes* 54, S40–S45. doi: 10.2337/diabetes.54.suppl_2.S40

Ybarra, J., Behrooz, A., Gabriel, A., Koseoglu, M. H., and Ismail-Beigi, F. (1997). Glycemia-lowering effect of cobalt chloride in the diabetic rat: increased GLUT1 mRNA expression. *Mol. Cell. Endocrinol.* 133, 151–160. doi: 10.1016/S0303-7207(97)00162-7

Zhong, Z., Liu, L. J., Dong, Z. Q., Lu, L., Wang, M., Leung, C. H., et al. (2015). Structure-based discovery of an immunomodulatory inhibitor of TLR1–TLR2 heterodimerization from a natural product-like database. *Chem. Commun.* 51, 11178–11181. doi: 10.1039/C5CC02728D

Conflict of Interest Statement: The authors declare that the research was conducted in the absence of any commercial or financial relationships that could be construed as a potential conflict of interest.